Chapter 9

# Thermoelectrics, Photovoltaics and Thermal Photovoltaics for Powering ICT Devices and Systems

Lourdes Ferre Llin and Douglas J. Paul

Additional information is available at the end of the chapter

http://dx.doi.org/10.5772/65983

**Abstract**

The conversion of heat into electricity through the thermoelectric effect and light into electricity through photovoltaic solar cells both allow useful amounts of power for a range of ICT systems from a few milli-Watts (mW) for autonomous sensors up to kilo-Watts (kW) for complete ICT computing or entertainment systems. Photovoltaics at the large scale can also be used to produce MW power stations suitable for the sustainable powering of high-performance computing (HPC) and dataservers for cloud computing. This chapter provides a background to the physics of operation of both types of sustainable energy sources along with the fundamental limits of both technologies. The present performance is presented along with promising research directions to allow for a comparison of the useful power along with the limits for deployment of each approach to power ICT devices and systems. Finally, the developing field of thermal photovoltaics is reviewed, where the overall thermodynamic conversion efficiency of turning light into electricity and useful heat can be increased through the addition of thermoelectrics or heat transfer modules to a photovoltaic cell.

**Keywords:** thermoelectrics, photovoltaics, energy harvesting

## 1. From heat to electricity: the thermoelectric effect

The increasing demand for energy has generated large amounts of carbon emissions from fossil fuels which has lead to climate change on the planet. This has made it necessary to identify new strategies to improve energy use and generation [1] which reduce the carbon dioxide emissions. Energy harvesting has become a significant field to take advantage of any free energy that is available from the environment or is waste from a system in order to recover that energy and use it for a wide range of applications. The environmental discussion of energy harvesting does not consist solely in replacing large-scale power stations and reducing their significant pollution when using coal or gas, but it also considers the use of powering smaller scale electronic devices. The idea of energy harvesting is by powering a lot of small devices, the

number of large power stations can be reduced thereby reducing carbon emissions. There are other benefits too: the major one is never having to worry about recharging batteries as the harvester is constantly harvesting energy.

Thermoelectric devices are able to deliver electricity to a load using heat as a power source or to produce heating or cooling in the presence of an electrical current. The Seebeck effect converts thermal energy into electrical energy, which makes this technology suitable for harvesting energy.

The Seebeck effect was first reported by Thomas Johann Seebeck in 1821, when he observed that when two electrical conductors were brought together, and the junction between them was heated up, a small voltage reading was sensed. This effect was proportional to a constant for any material called the Seebeck coefficient ($\alpha$) which was defined as the ratio between the voltage sensed ($\Delta V$) and the existent gradient of temperature ($\Delta T$), as define in Eq. (1)

$$\alpha = \frac{\Delta V}{\Delta T}. \tag{1}$$

Thirteen years later, in 1834, Jean Charles Athanase Peltier discovered that when an electrical current was driven through a thermocouple, a small heating or cooling was produced depending of the direction of this current. This effect, named as the Peltier effect ($\Pi$), was defined as the ratio between the heating or cooling rate at each junction ($Q$) and the current passing through it ($I$), as reported in Eq. (2)

$$\Pi = \frac{Q}{I}. \tag{2}$$

In 1855, William Thomson (Lord Kelvin) recognised the relation between the two effects explained above. These Kelvin relations demonstrated the reversible heating or cooling when there was an electrical current flowing in addition to a gradient of temperature. The relation between the Seebeck and the Peltier effect was given by

$$\Pi = \alpha T. \tag{3}$$

The Thomson effect ($\tau$) was defined as the rate of heating or cooling per unit length through a junction, where there existed a unit current and a unit gradient of temperature. This effect was also related to the Seebeck effect by

$$\tau = T\frac{d\alpha}{dT}. \tag{4}$$

In 1911, Edmund Altenkirch derived the efficiency of the thermoelectric generation process, stating the different qualities required to define a good thermoelectric material, which will be described later in this chapter. Interest in exploiting thermoelectric phenomena for power generation began during the late nineteenth and twentieth century, and in the 1950s, the study of semiconductor materials became very interesting for the construction of thermoelectric generators, as well as practical Peltier coolers.

http://dx.doi.org/10.5772/65983

As the Seebeck effect is responsible for power generation, a more detailed explanation of it is given in the following section, as well as other parameters which define the efficiency of a thermoelectric system. Following this definition, a review of the different materials and approaches used during the past and present years to achieve improvements in the Seebeck coefficient is reported.

### 1.1. Thermoelectric power generation

Let us consider a pair of semiconductor legs (p-type and n-type) connected electrically in series and thermally in parallel. If one side of the pair of legs is heated up and the other side is kept at a reference temperature, the $\Delta T$ between the two sides produces excess carriers which may diffuse from the hot to the cold side. This diffusion of carriers sets the Seebeck voltage which will deliver a current ($I$) when the circuit is closed with a load, as shown in **Figure 1**.

The efficiency of the system ($\eta$) is therefore given by the ratio of the output power, $P$ to the rate of the heat that is drawn from the source, $\eta = \frac{P}{Q}$. The current flowing through the circuit is given by

$$I = \frac{(\alpha_p - \alpha_n)(T_1 - T_2)}{R_L + R_p + R_n}, \tag{5}$$

where $R_p$ and $R_n$ are the resistances of each semiconductor material (p-type and n-type), $R_L$ is the resistance of the load and $\alpha_p$ and $\alpha_n$ are the Seebeck coefficients of each leg, respectively [2]. The power delivered to the load resistor is given by Eq. (6) [2]

$$P = \left(\frac{(\alpha_p - \alpha_n)(T_1 - T_2)}{R_L + R_p + R_n}\right)^2 R_L. \tag{6}$$

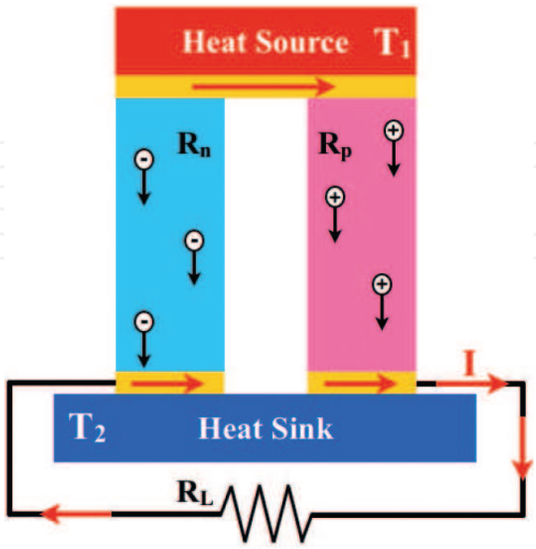


**Figure 1.** A schematic diagram of a module formed by a pair of thermoelectric legs connected electrically in series and thermally in parallel. The circuit has been closed, connecting a resistor across the module.

On the other hand, the heat that is drawn from the source is defined by

$$Q = (\alpha_p - \alpha_n) I T_1 + (\kappa_p + \kappa_n)(T_1 - T_2), \tag{7}$$

where $\kappa_p$ and $\kappa_n$ are the thermal conductances of the two legs [2].

The efficiency reaches its maximum when [2]:

$$\frac{R_L}{R_n + R_p} = \sqrt{1 + ZT} \quad \text{where} \quad ZT = \frac{\alpha^2 \sigma}{\kappa} T, \tag{8}$$

where $\sigma = \sigma_n + \sigma_p$ $(S/m)$ is the electrical conductivity, $\alpha = \alpha_p - \alpha_n$ $(\mu$ V/K) is the Seebeck coefficient and $\kappa = \kappa_p + \kappa_n$ (W/mK) is the thermal conductivity of the material.

Using Eq. (8) in Eqs. (6) and (7), the efficiency can be defined by the following expression [2]:

$$\eta = \frac{T_1 - T_2}{T_1} \frac{\sqrt{1 + ZT} - 1}{\sqrt{1 + ZT} + \frac{T_2}{T_1}}. \tag{9}$$

From the efficiency, it is shown that if ZT is much larger than unity, the model approaches the Carnot efficiency given by $(T_1\text{-}T_2)/T_1$. **Figure 2** shows the efficiency given for different values of ZT, where the system approaches the Carnot efficiency each time the value of ZT becomes

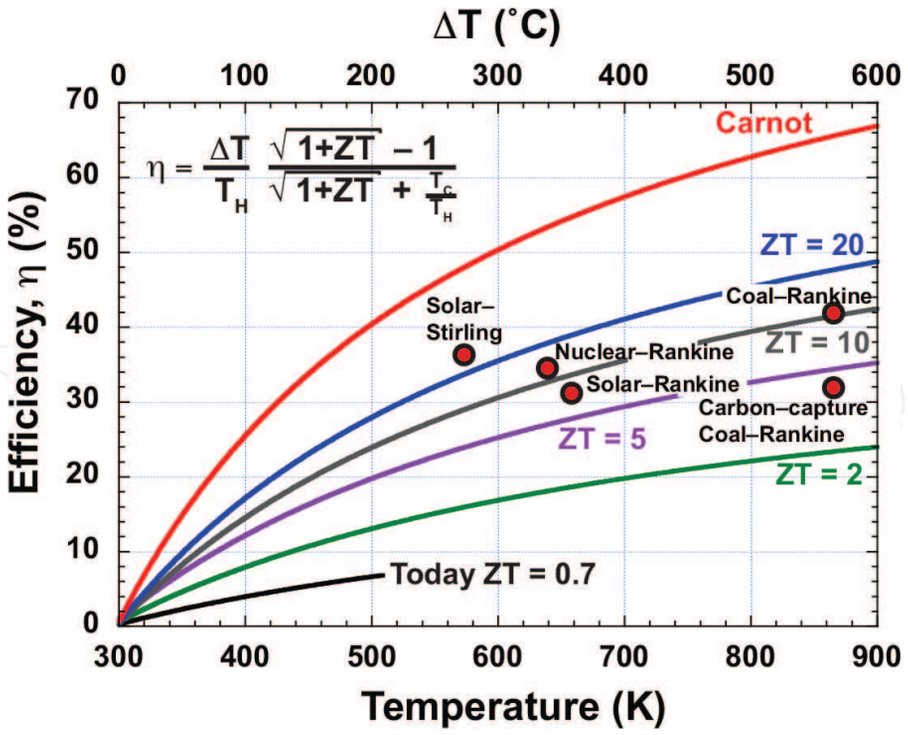


**Figure 2.** A plot showing the maximum thermoelectric efficiency for different ZT values. These values have been compared to the Carnot efficiency, also plotted in the figure. Also presented are the efficiencies of other technologies as a comparison.

http://dx.doi.org/10.5772/65983

larger. Therefore, ZT is known as the figure of merit that defines the efficiency of a thermoelectric material.

Until now, we have only considered two legs connected to a load, but a real thermoelectric generator (TEG) features several of these thermoelectric couples electrically connected in series. As the Seebeck coefficients of most materials used for thermoelectric generators are of order of 100–200 μV/K, a large number of these legs has to be connected electrically in series and thermally in parallel to generate useful voltages, > 1 V, to be able to power electronics such as ICT systems. **Figure 3** shows a diagram of a full module where several thermoelectric couples are connected electrically in series and thermally in parallel.

Getting the maximum efficiency out of a module does not mean generating the maximum power output; in fact, the power output reaches its maximum when there is electrical impedance matching between the generator and the load which occurs when $R_L=R_n + R_p$. Taking this into account, and using the relation given by Eq. (6), one gets that $P_{max}$ is defined by

$$P_{max} = \frac{1}{2} NF \frac{A}{L} \Delta T^2 \alpha^2 \sigma, \tag{10}$$

where N is the number of legs, F is the fabrication factor and A and L are the area and the length of the legs, respectively (see **Figure 3**) [3]. The fabrication factor denotes the perfect system, where there are not losses of any kind, to account for contact resistances and wasted heat.

When characterising a material, apart from its efficiency, it is also important to consider separately the relation $\alpha^2\sigma$. This is the second figure of merit of a thermoelectric material and represents the output power of the system, also known as the *Power Factor*.

Current research efforts are focusing on finding new materials that can increase the efficiency (ZT) together with the power factor ($\alpha^2\sigma$) of thermoelectric devices, and that can also operate

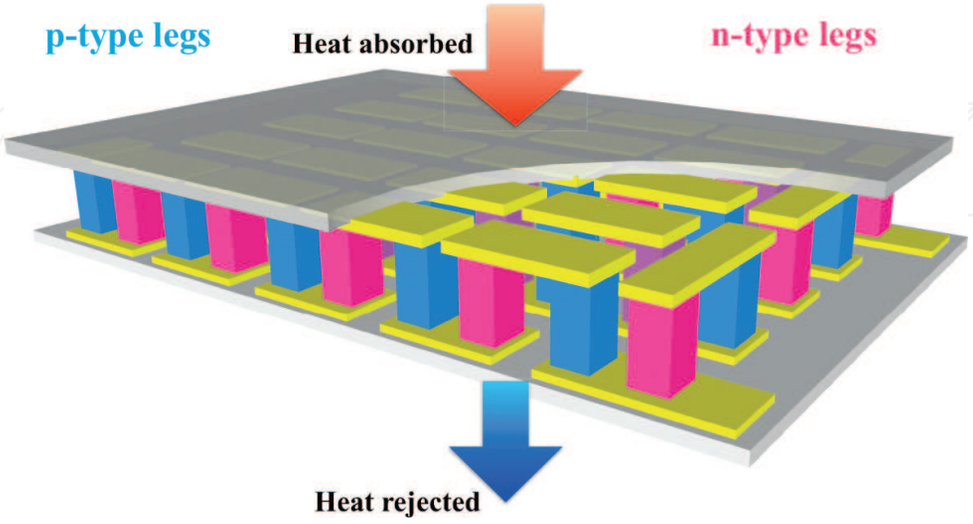


**Figure 3.** A schematic diagram of a thermoelectric module where the p-type and n-type legs have been bonded together, connecting them electrically in series and thermally in parallel.

over wider temperature ranges. Over the last decades, bismuth telluride and silicon-germanium materials have been extensively studied, as BiTe- and SiGe-based systems have shown the highest efficiencies at room temperatures (300K) and high temperatures (1100K), respectively. These platform materials are currently used in many applications, and therefore, there is significant interest in finding new materials that would be more efficient. Some research groups have been working with low-dimensional systems such as superlattices, nanowires and quantum dots, to demonstrate a new way to improve $\alpha$, $\sigma$ and $\kappa$; however, improving these parameters at the same time has been shown to be very challenging. A lot of effort has been undertaken to drastically decrease the thermal conductivity, which as a consequence had a good improvement of ZT, but did not necessarily mean that the power output was increased as well. In fact, it is usually found in the literature that even though the value of ZT has improved, the power factor has decreased due to the reduction in the electrical impedance matching between the generator and the load, which makes it very difficult for this material to be implemented in real applications.

**Figure 4** shows a comparison of the best n-type and p-type ZT values as a function of temperature. The solid lines show the ZT values for bulk materials, where most of them present values around 1 or less than 1. The dashed lines present the values reported in the literature for low-dimensional structures where quantum effects or nanostructures can be used to optimise the ZT. The approach is always to find quantum effects or nanostructures that can scatter heat in the quantised form of phonons more efficiently than electrons, so the thermal conductivity reduces faster than the electrical conductivity. In 3D, this is nearly impossible due to the Wiedemann-Franz rule, but in low-dimensional systems, it is possible to break the linear relationship between the electrical and thermal conductivities at high carrier densities and therefore increasing ZT.

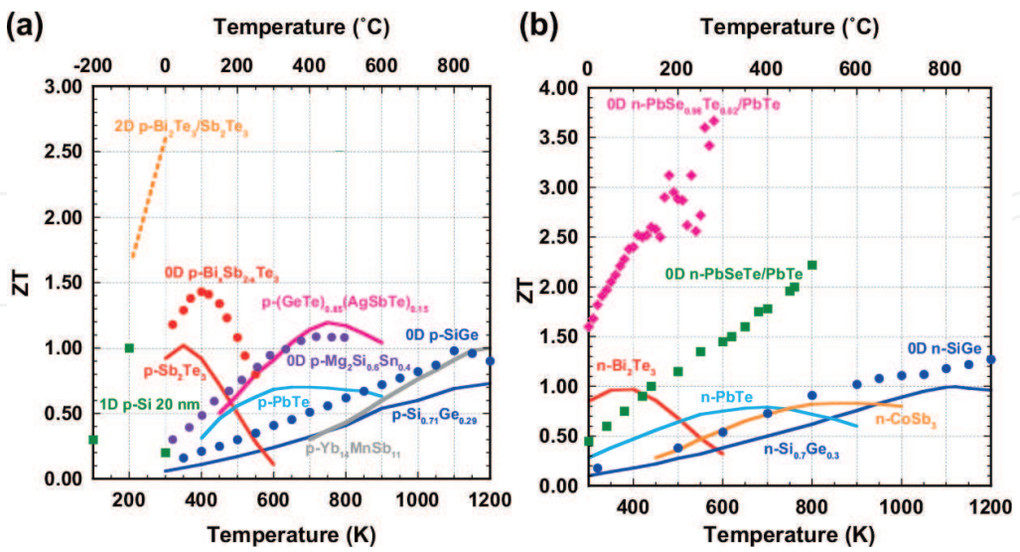


**Figure 4.** Left: a comparison of ZT for p-type material as a function of temperature (p-$Sb_2Te_3$, p-PbTe, p-$CeFe_4Sb_{12}$, p-$Yb_{14}MnSb_{11}$ [4], p-$Si_{0.71}Ge_{0.29}$ [5], 2D p-$Bi_2Te_3/Sb_2Te_3$ [6], 1D Si [7], 0D p-SiGe [8], p-$(GeTe)_{0.85}$ $(AgSbTe)_{0.15}$ [3], 0D p-$BixSb_{2-x}Te_3$ [9], 0D $Mg_2Si_{0.4}Sn_{0.6}$ [10]). Right: a comparison of ZT for n-type material as a function of temperature (n-$Bi_2Te_3$, n-PbTe, n-$CoSb_3$ [4], n-$Si_{0.7}Ge_{0.3}$ [5], 0D PbSeTe [11], 0D n-SiGe [12], 0D n-$PbSe_{0.98}Te_{0.02}$/PbTe [13]).

http://dx.doi.org/10.5772/65983

## 1.2. Applications

Thermoelectric generators are robust, do not have moving parts, do not require maintenance and can generate continuous power as long as there is a heat source. Therefore, this technology is an attractive way to recover wasted heat rejected into the environment and is normally a fit and forget technology.

Thermoelectric generators can be used over a wide range of temperatures, which makes them useful in many different systems. In the following list, there are some of the applications mentioned where thermoelectric generators are currently used or are under investigation.

### *1.2.1. Applications close to room temperature*

- Implantable medical devices have the disadvantage of depending on batteries, with life times ranging from 5 to 10 years. These devices could be powered by using temperature differences that exist between the inner surface of the skin and the body core. A thermoelectric module generating around 70 μW in the presence of these temperature gradients could be useful in these applications [15].
- The major application for thermoelectric devices at present is as Peltier coolers (**Figure 5** left) to maintain electronic and optoelectronic components at stable temperatures. For instance, laser diodes are kept at a constant temperature by Peltier coolers to obtain a constant emission wavelength for telecoms applications. Other applications, such as DNA amplifiers for cell imaging, have a strong reaction sensitivity to temperature, and therefore, Peltier elements are used not only for temperature stability but also to enable a large range of temperatures that they can provide. Thermoelectric cooling is also used in the automotive industry to cool down the batteries of electric cars when these are charging.
- Wireless sensors are autonomous devices combining sensing, power, computation and communication into one system; smartdust has become a term to refer to these kind of sensors. Most wireless sensors systems now require between 1 and 5 mW of power to run mainly dependent on the distance for the communication, and so a $cm^2$ area thermoelectric

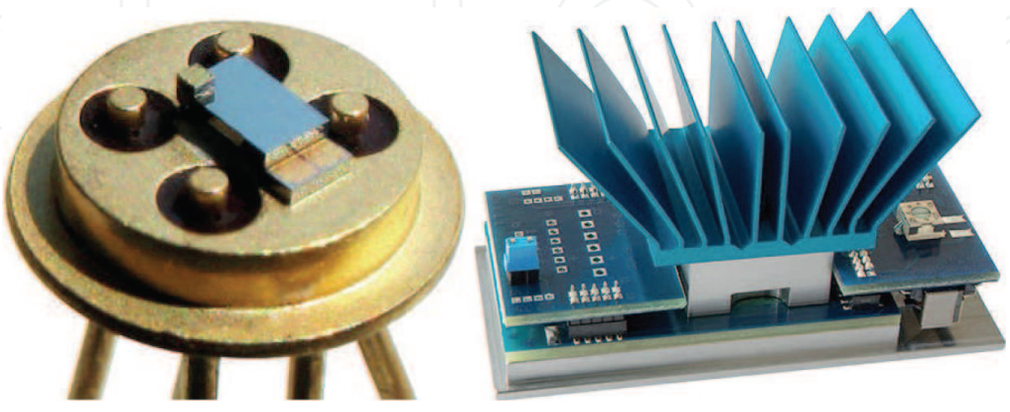

**Figure 5.** Left: A telecoms laser on a microfabricated Peltier cooler produced by Micropelt. Right: A thermoelectric generator produced by Micropelt showing the cold sink aimed at dissipating heat through air cooling. copyright Micropelt [14].

device requires around 50°C to provide sufficient power. As the communications consume the most power, most systems have rechargeable battery or super-capacitor storage systems and then use burst modes of communication so that information is only sent when required thereby minimising the power consumption. Therefore, it is the cost of replacing batteries (mainly labour costs) that allows thermoelectrics and other forms of energy harvesting to be cost-effective. As an example, EnOcean described how after installing 4200 energy harvesters to power light switches, occupancy sensors and daylight sensors in a new building, they had saved 40% of lighting energy costs, 20 miles in cables and 42,000 batteries (over 25 years), and as a consequence, they had reduced the amount of toxins released by batteries to the environment [1]. The right image in **Figure 5** shows a thermoelectric generator embedded onto a circuit board to collect part of the heat generated by the electronics and convert it into useful power.

### *1.2.2. High-temperature and industrial applications*

- The largest driver for improved thermoelectrics at present is probably the car industry where European legislation to improve fuel efficiency is driving thermoelectrics research to replace the alternator. The car is a system where thermoelectrics could play a big role as 75% of the fuel ends up as waste heat and the 40% of waste heat goes down the exhaust pipe into an environment that could be used to capture this heat and convert it into electricity, as shown in (**Figure 6**) [3, 6, 16]. The temperature of the exhaust system can range from room temperature up to 750°C, so this is driving work on new thermoelectric materials to replace the best at present which is PbTe with toxic Pb that cannot be used for applications. Initial modelling has suggested that up to a 5% in fuel consumption could be achieved with suitable thermoelectrics with ZT of 1, but the key issue is getting the whole

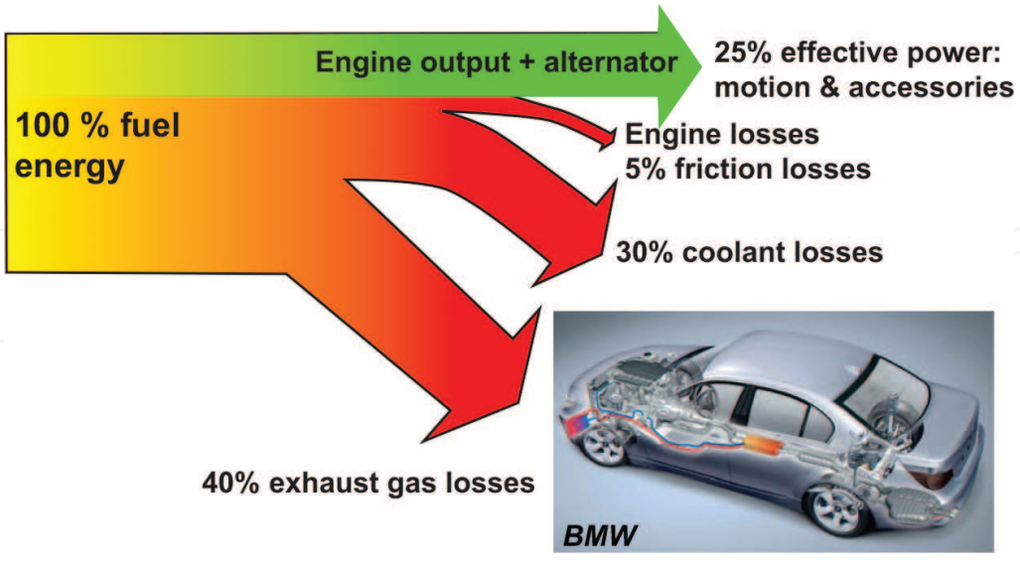


**Figure 6.** A schematic diagram of how the energy from a combustion engine in a car is distributed. 25% of the energy produces motion and through the alternator generates electricity to power accessories including the electrics, the air conditioning and the hifi system. 75% of the energy from the fuel is lost mostly through friction and heat. 40% of the fuel energy disappears through the exhaust system; hence, there is interest in using thermoelectrics to harvest some of this waste energy.

http://dx.doi.org/10.5772/65983

thermoelectric system cheap enough for the market. Also, no thermoelectric provides ZT of 1 from room temperature to 750°C, so segmented modules and/or new materials are required. Most of the major car companies are now working heavily of thermoelectric, and it is only a mater of time before automotive systems become available.

- Due to the absence of vibration, noise or torque during operation, thermoelectric generators are suitable systems for powering space missions [3]. Space systems use radioisotope thermoelectric generators (RTGs) where a radioactive material heated by the decay, and emission of radiation is used as the hot source with a thermoelectric generator to turn the heat into electricity. These systems typically operate close to 1000°C, and because of these high temperatures, SiGe has been the main thermoelectric material used for these generators, reaching efficiencies as high as 6.6%. Therefore, this is the major reason NASA used radioisotope thermoelectric generators for the Voyager space probes which have been operating for over 34 years and have now left the solar system.

## 2. From light to electricity: the photovoltaic effect

Solar cells are semiconductor devices which are able to convert solar energy into electricity [17], using the photovoltaic (PV) effect which is responsible for this conversion. When a p-n junction formed by a semiconductor material is exposed to an electromagnetic radiation, such as light, photons with sufficient energy will excite electrons from the valence band to the conduction band leaving a hole behind. Due to the built-in asymmetry of the device, the excited electrons and holes will be separated away to an external circuit to create an electrical current [18]. The efficiency of a PV device depends on the light absorbed by the material and also on the electrical connections to the external circuit.

The PV effect was discovered by Edmund Becquerel in 1839, who observed that a small electrical current was generated after exposing an electrode to light which was immersed in an electrolyte solution [19]. Some years later, in 1877, William Adams and Richard Day built the first solar cell, which consisted of a selenium sample with two platinum contacts on it [20].

The efficiency of these first devices, however, was still too poor for any applications, and therefore, it was necessary to wait many decades in order to have a better understanding of semiconductor materials. In 1947, William Shockley, John Bardeen and Walter Brattain developed the first germanium transistor [21], which led to a method to fabricate p-n junctions, first in germanium and later in silicon, with better photovoltaic behaviour. In 1954, Chapin, Fuller and Pearson developed the first silicon solar cell in the Bell Telephone laboratories. This solar cell was the first photovoltaic device to convert light into electrical work with an efficiency of 6% [22]. The interest in solar cells drastically increased due to the oil crisis in the 1970s. Alternative energy sources were required, and therefore, a lot of funding was invested into solar energy development.

At first, solar cells were only used for space applications, but soon, the efficiency and cost of silicon solar cells were improved to the point which made possible their use in many terrestrial

applications. Other semiconductor materials, such as GaAs, and thin film technologies were investigated, as well as new structures with multiples junctions to widen the absorption of radiation and hence improving the efficiency of these devices.

During this period, new structures were developed to improve the efficiency of these PV devices. Some of the structures that are still currently in use are the development of thinner junctions to improve the absorption of ultraviolet light and the development of textured surfaces as well as antireflective coatings to decrease the losses due to the reflection of light [23].

In the 1980s, silicon solar cells with efficiencies around 20% were first fabricated. Currently, silicon is the cheapest, most abundant and available semiconductor material with a useful PV efficiency, and therefore, it is the most used material for terrestrial applications. In 2014, 35% of the PV market used crystalline silicon and 56% of the market used poly-crystalline silicon which combined account for 91% of the overall PV market [24]. The remaining 9% of the market is from thin film technologies which includes amorphous silicon and CdTe. The development of new manufacture technologies, however, as well as the investigation of new materials that could improve the efficiency and reduces the cost are still in development.

### 2.1. Available solar energy

The sun emits light within a range of wavelengths where three regions can be differentiated: the ultraviolet, visible and infrared region of the electromagnetic spectrum, see **Figure 7** (left). **Figure 7** (right) shows the solar irradiance as a function of wavelength at a point outside the Earth's atmosphere (AM0, blue line), which corresponds approximately to the radiation of a black body with a temperature of 5760 K [also shown in **Figure 7** (right, black line)]. The sun (with a temperature of 5760 K) presents its strongest emission at visible wavelengths, reaching its peak inside the blue-green region.

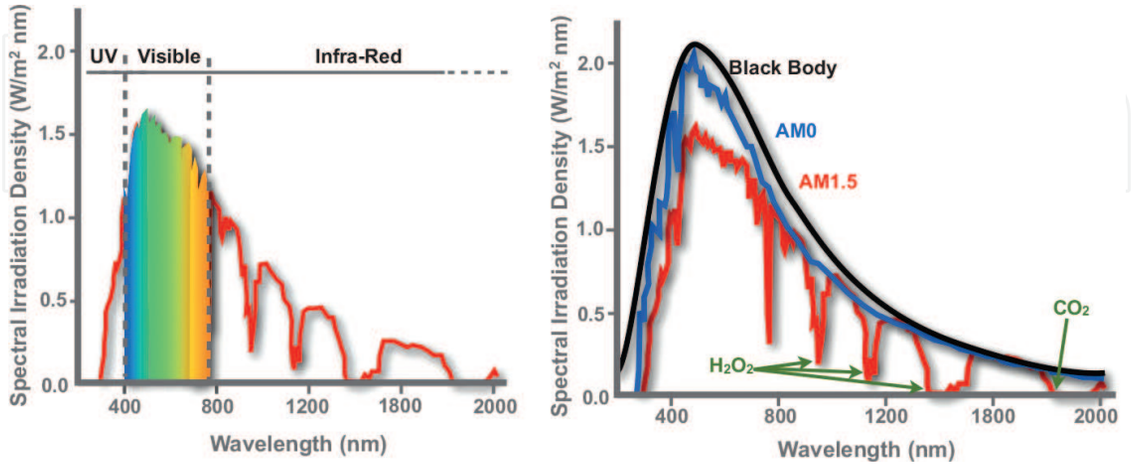


**Figure 7.** Left: spectral irradiation density at AM1.5 versus different wavelengths, showing the UV, visible and infrared region. Right: spectral irradiation density versus different wavelengths for AM0 and AM1.5, and for a black body with a temperature of 5760 K.

http://dx.doi.org/10.5772/65983

As solar energy travels through the atmosphere, light is absorbed by many of its elements. In fact, some of these elements can be identified by their absorption lines (Fraunhofer lines). As an example, water and $CO_2$ are mainly absorb in the infrared region, being responsible for some of the absorption dips in the spectrum showed in **Figure 7** (right, AM1, red line).

The attenuation caused by the light traveling through the atmosphere is defined by the 'Air Mass' index, which is defined as:

$$n_{AirMass} = \frac{\text{optical path length to sun}}{\text{optical path length if sun directly overhead}} = \frac{1}{cos(\gamma)} \tag{11}$$

where $\gamma$ (see **Figure 8**) is the angle between the optical path length of sun and the normal through a horizontal plan at the point of observation.

As the spectrum of light changes depending on the day and the location, a standard reference for the spectra is defined in order to perform valid comparison of PV devices within the different research institutes and companies. For terrestrial use, the standard reference is defined for an air mass of AM1.5, which corresponds to an angle of elevation for the sun of 42° which is a latitude of 37°, and to an irradiance of 1000 $Wm^{-2}$.

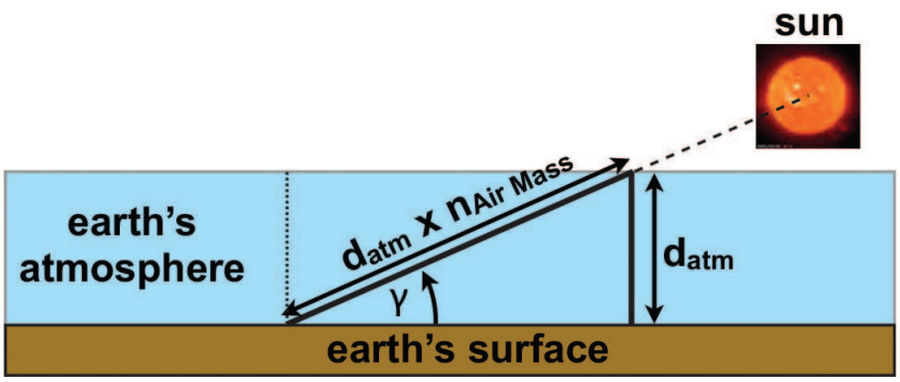


**Figure 8.** A schematic diagram showing the atmospheric attenuation and how the air mass index is calculated.

## 2.2. P-N junction

Semiconductor materials are used in order to take advantage of the electromagnetic radiation that comes from the sun to convert part of this energy into electricity (the photovoltaic effect). The physics for this effect to take place inside a material is based on the p-n junction, and the junction between two semiconductor materials doped n-type and p-type [18, 25].

In a semiconductor material, the lower energy level (valence band, $E_v$) is separated from the energy level where an electron can be considered free (conduction band, $E_c$), by an energy gap known as the band gap ($E_g$). When the semiconductor material is exposed to a flux of light, photons can be either reflected, absorbed or transmitted, see **Figure 9** (left). If the photons are reflected or transmitted, then they will be lost into the environment without contributing to the PV current. On the other hand, if they are absorbed by the material [**Figure 9** (right)], only

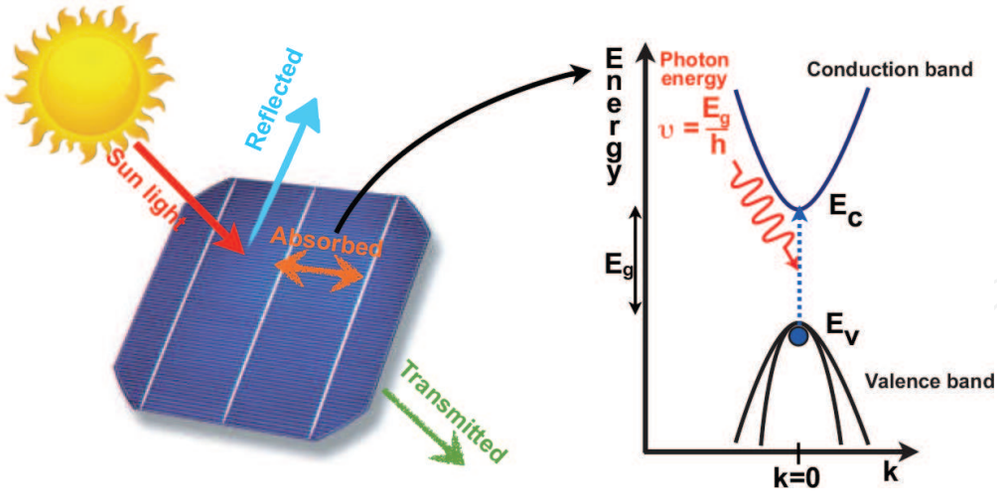


**Figure 9.** Left: A schematic diagram showing how the light can be either reflected, transmitted or absorbed by a solar cell. Right: Only photons which are absorbed can contribute to electron-hole generation. A photon with a greater energy than $E_g$ can excite an electron from the $E_V$ to $E_C$.

photons with a frequency $\upsilon$ corresponding to an energy ($h\upsilon \geq E_g$) equal or greater than the band gap will be able to excite an electron from the valence band into the conduction band, and therefore contribute to the PV current.

The concentration of electrons inside the conduction band and the concentration of holes inside the valence band can be controlled by the addition of impurities into the material. These impurities are considered either as donors ($N_D$), which increase the concentration of electrons inside the conduction band, or acceptors ($N_A$), which increase the concentration of holes inside the valence band. If the concentration of electrons is higher than the concentration of holes, then the current is dominated by the movement of electrons, and the semiconductor is considered as n-type. On the other hand, if the current is dominated by the movement of holes, then the semiconductor will be considered as p-type.

If a photon has enough energy to create an electron-hole pair, then there is a high possibility for the carriers to be separated by the electric field generated by the p-n junction, which will contribute to generate an electric current once the device is connected to a load (**Figure 10**). In reality, a p-n junction only provides a very small depth inside the depletion region for absorption so to increase the absorption depth of the PV cell, p-i-n junctions are formed with a large undoped i absorption region between the two doped regions. There is also a possibility for the excited electron to recombine with a hole inside the valence band before the electric field can drive away the carriers. This process is known as recombination, and it is a loss mechanism for solar cells as the generated electron hole pair is re-emitted as light from the cell.

The distance that a photon can travel inside the material before it is absorbed is defined as the absorption coefficient ($\alpha$), Eq. (12):

$$\alpha = \frac{4\pi\kappa}{\lambda} \tag{12}$$

http://dx.doi.org/10.5772/65983

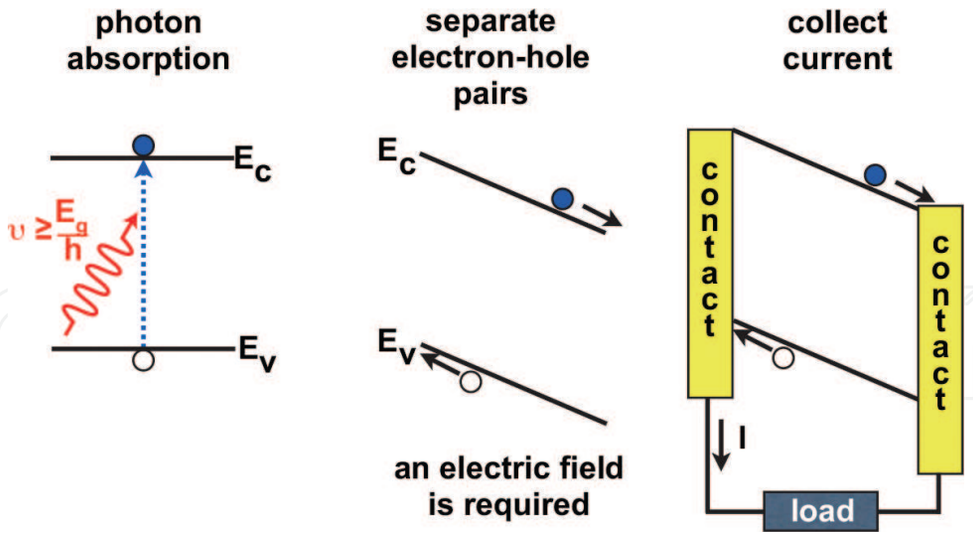


**Figure 10.** A schematic diagram showing a sequence of steps (from right to left) from photon absorption into the material, to electron-hole pair generation and to collection of current into an external circuit.

where $\kappa$ is the extinction coefficient and $\lambda$ is the wavelength. The absorption coefficient not only depends on the material, but also on the wavelength at which light is to be absorbed. For instance, if the material is too thin, photons with high wavelength will be transmitted as if the material was transparent to them. **Figure 11** shows the absorption coefficient values as well as the penetration depth $(1/\alpha)$ into the material as a function of photon energy for a range of semiconductor materials typically used to make PV cells. Whilst Si is the material which dominates the PV market, it can be observed that it does not have the best absorption coefficients for PV cells. Ge, InP and GaAs have better absorption coefficients for a given photon

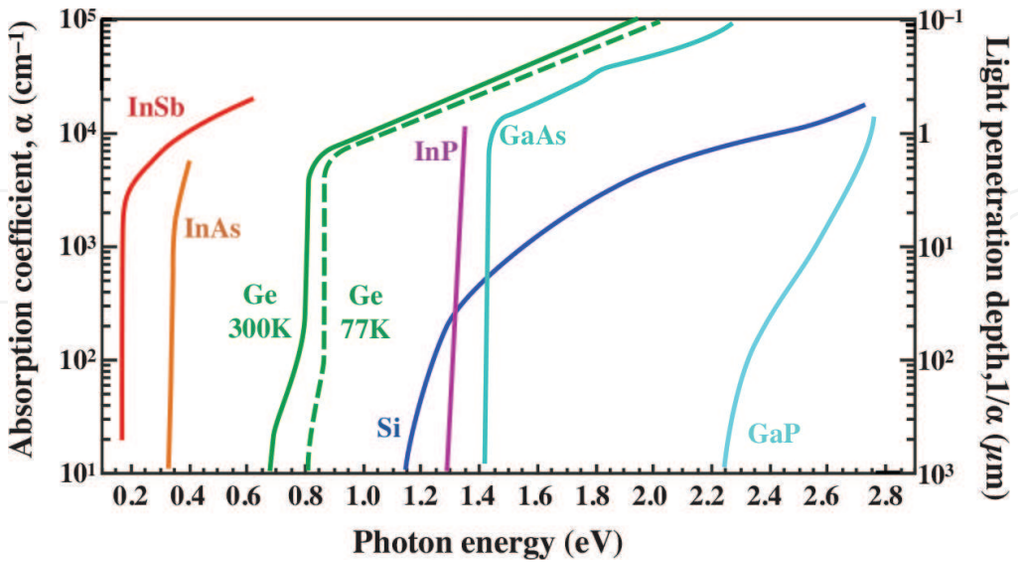


**Figure 11.** Absorption coefficient and penetration depth values as a function of photon energy for different semiconductors.

energy allowing less material, but Si dominates because it is one of the cheapest and most plentiful material available in the semiconductor industry.

### 2.3. Circuit model of p-n photovoltaic solar cell and the efficiency

A photovoltaic device is based on a semiconductor material p-n or p-i-n junction where an asymmetric junction is required in order to separate the carriers. Most of these devices behave as a diode in the dark, where the device admits more current under a forwarded voltage than at a reversed voltage. Therefore, it can be said that a solar cell behaves as a current source with a diode connected in parallel [see **Figure 12** (left)].

When the solar cell is not connected to a load (open circuit), most of the generated current flows through the diode, which is known as the dark current. The dark current is equivalent to the current that would flow through the circuit if an external voltage was applied to the cell in the dark. Eqs. (13) and (14) define the current ($J_{dark}$) and voltage ($V_{oc}$) when the device is in open circuit

$$J_{dark} = J_0(e^{qV/k_BT} - 1) \tag{13}$$

$$V_{oc} = \frac{k_BT}{q}\ln(\frac{J_{sc}}{I_0} + 1) \tag{14}$$

where $J_0$ is a constant, $k_B$ is the Boltzmann's constant, $T$ is the temperature and $J_{sc}$ is the short-circuit current. As an approximation, the current-voltage characteristic is the superposition of the dark current plus the short circuit photocurrent [$J_{sc}$ **Figure 12** (right)].

Looking at the equivalent electrical circuit represented in **Figure 12**, the total current density is given by

$$J_V = J_{sc} - J_{dark}(V), \tag{15}$$

which becomes the following expression for an ideal diode,

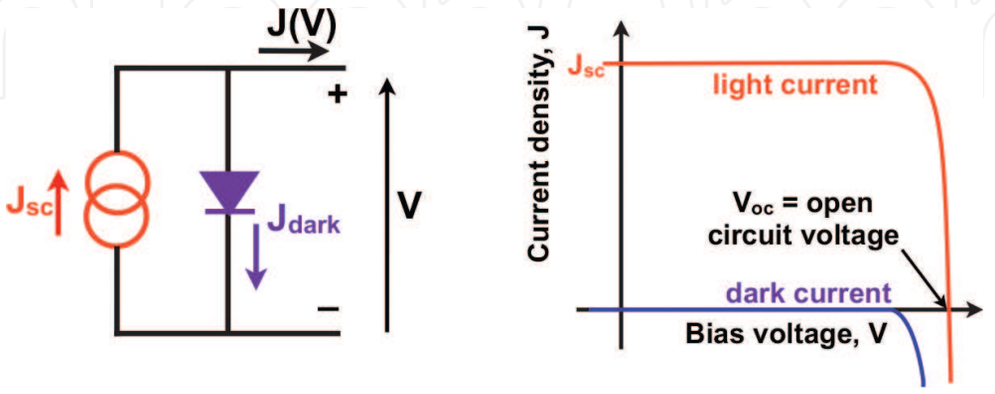


**Figure 12.** Circuit model for a solar cell. The devices behave as a current source with a diode connected in parallel.

http://dx.doi.org/10.5772/65983

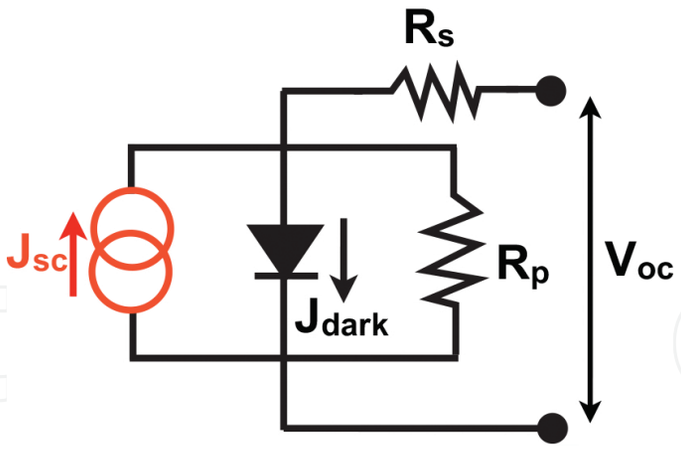


**Figure 13.** The circuit model for a real solar cell, where the series resistances due to the contacts and the parallel resistances due to the p-n junction have been added.

$$J_V = J_{sc} - J_0(e^{qV/k_BT} - 1). \tag{16}$$

Until now, we have only discussed ideal PV devices, but unfortunately, real solar cells present two parasitic resistances which degrade the performance of these devices. **Figure 13** shows the equivalent electrical circuit for a real solar cell, where there is a series resistance ($R_s$) and a parallel resistance ($R_p$). $R_s$ is related to the series resistances created by the front and back contacts between the metal and semiconductor and also due to the interconnects used for connecting the electrical circuit. $R_p$ is related to the leakage current of the cell around the edges of the device, and it also shows the quality of the p-n junction.

The power density of a solar cell is given by

$$P = JV. \tag{17}$$

The maximum power density for a photovoltaic device occurs at a certain $V_m$ and $I_m$, which does not correspond to the maximum current or voltage provided by the device, see **Figure 14**. Therefore, the fill factor (FF) is defined as the fraction between the maximum power that the solar cell can deliver to a load, and the theoretical maximum power density defined by $J_{sc}$ and $V_{oc}$

$$FF = \frac{V_m J_m}{V_{oc} J_{sc}}. \tag{18}$$

The more the FF approximates to 1, the more the power density approaches to the theoretical value. The efficiency then can be defined as the maximum power that a solar cell can deliver to a load at an operating point $P_m$ versus the incident light power density $P_s$

$$\eta = \frac{P_m}{P_s} = \frac{FFV_{oc}I_{sc}}{P_s}. \tag{19}$$

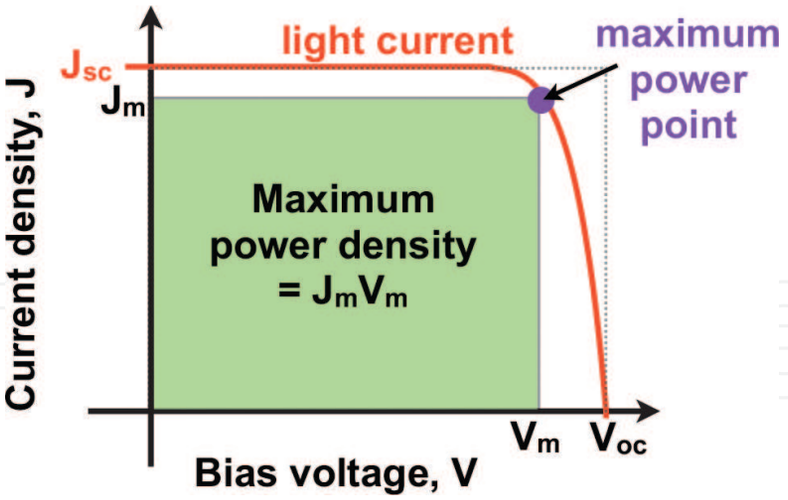


**Figure 14.** Schematic diagram showing the maximum power point of a solar cell, which does not match with the theoretical maximum power density.

Therefore, $J_{sc}$, $V_{oc}$, FF and $\eta$ are the parameters evaluated to define the quality of a solar cell. As explained in Section2.1, solar cell is normally tested in laboratories following the AM1.5 spectrum, with an incident light power density of 1000 W m$^{-2}$ and a temperature of 25°C.

**Figure 15** shows the current density values versus the open-circuit voltage values for different semiconductor materials.

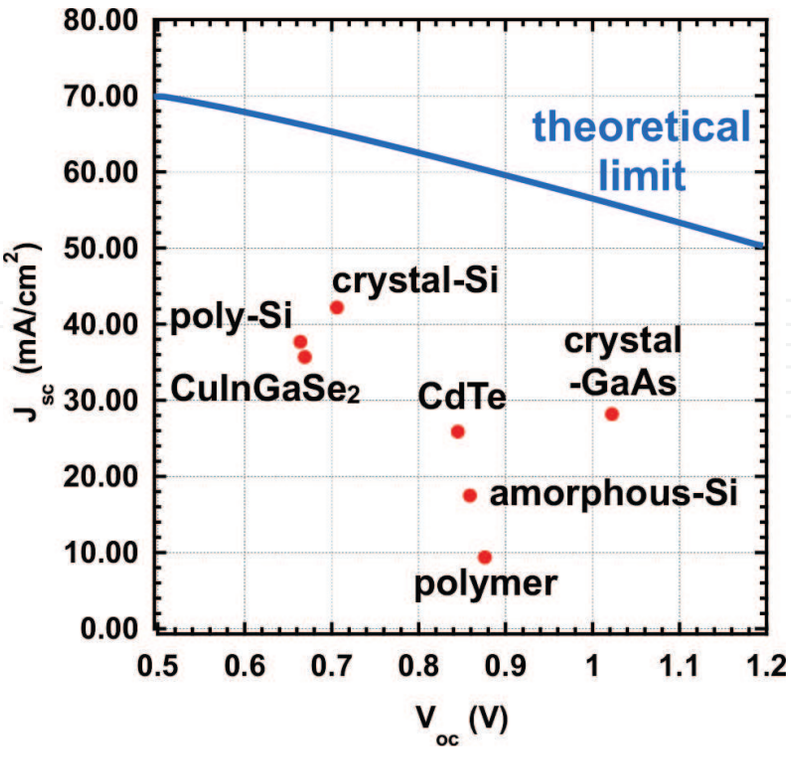


**Figure 15.** Graph showing the current density values as a function of $V_{oc}$ for different semiconductor materials.

http://dx.doi.org/10.5772/65983

### 2.4. PV efficiency

The Carnot efficiency of a PV cell can be calculated by considering the PV cell as a perfect blackbody absorber. Since the sun emits a blackbody spectrum with a temperature corresponding to 5760K, it can be demonstrated that the maximum absorption occurs when the PV cell as a blackbody absorber is at 2470K. The Carnot efficiency is 85% when all the photons are absorbed, and each absorbed photon generates the maximum amount of heat available from the photon, and there is zero thermal dissipation from the absorber. Of course, no real PV cell can be operated at 2470K, and many of these approximations are not true in the real world so all efficiencies will be lower than this number.

A more practical efficiency is for a PV cell which produced from a single semiconductor material. This was first calculated by Shockley and Quessier [26] in 1961. The calculation assumes a PV cell which emits as a blackbody and has no light incident and no applied voltage. The work then considers all the radiation which can be absorbed by the semiconductor with energies above the bandgap, $E_g$, and assumes only band-to-band recombination. Geometrical factors are added to work out the amount of light that can be absorbed by a flat PV cell and also to account for the temperature of the sun and the temperature of the PV cell. For PV cells at 300K, the maximum efficiency for a Si cell is 30% and for a GaAs cell is 31%. The Shockley-Quessier efficiency is a maximum for a bandgap of about 1.4eV and falls off for larger and smaller bandgaps. The best Si cell is 25.6%, and the best GaAs single cell is 28% for illumination with 1 sun [27], so these numbers are quite close to the Shockley-Quessier limit.

For any material, a number of optimisation strategies are employed in all PV cell manufacture to increase the performance and get close to the Shockley-Quessier limit. If a piece of flat silicon is used as a PV cell, then the maximum efficiency is around 13%, well below the record 25.6% efficiency [27]. Key to optimising the cell is to realise that not all the light from the sun enters the cell, and even if the light does enter the PV cell, not all of the photons will always be absorbed. The first approach is to texture the surface which increases the path length of the light inside the PV material if a metal reflector is deposited onto the back surface. The left side of **Figure 16** presents the concept of textured surfaces where the sunlight has the rays reflected when absorbed. The light is then reflected along with the material from a back reflector, and if

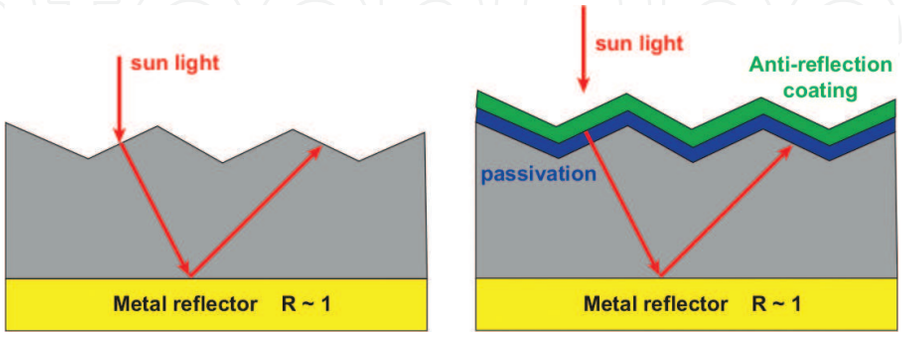


**Figure 16.** Schematic diagrams showing how a corrugated surface can be used to increase the path length of light in the solar cell and therefore increase the absorption of radiation. Left: a simple textured surface which increases the path length of light through refraction at the surface and a backside metal mirror. Right: the same correlation but with an additional anti-reflection coating to reduce the reflected light from the cell surface.

the correct angles are chosen for the texture, then total internal reflection can increase the path length to typically four times the thickness of the material. This is especially important for indirect bandgap materials such as silicon where the absorption coefficient (see **Figure 11**) can be quite low close to the bandgap edge.

The second key part of optimising a PV cell is surface passivation. Dangling bonds at the surface where the periodic crystal lattice is broken can trap the photo excited electron-hole pairs resulting in a reduction in the efficiency of the PV cell. Passivation is important to reduce the number of surface traps to provide the maximum efficiency. For Si PV cells, thermal silicon dioxide provides a very high-quality passivation where surface trap densities can be reduced to $\sim 10^{10}\,\mathrm{cm}^{-2}$ whilst such a low level of traps is difficult to achieve on other semiconductor materials.

Finally, an anti-reflection coating can significantly reduce the light that is reflected from the PV cell surface (see **Figure 11** right). The reflection $R$ from a surface is dependent on the refractive index of the cell material $n_{PV}$ and the refractive index of air which is $n_{air} \sim 1$. The reflection from the PV surface is given by

$$R = \left(\frac{n_{PV} - n_{air}}{n_{PV} + n_{air}}\right)^2. \tag{20}$$

For Si, $n_{PV} = 3.5$ and so 30% of the light is reflected from a silicon surface leaving only 70% of the sunlight able to be absorbed by the PV cell. The way to reduce the amount of light which is reflected is to add an anti-reflection coating. The reflection $R$ vanishes if a coating is deposited with an intermediate refractive index given by $n_{ARC} = \sqrt{n_{air} n_{PV}}$ with a thickness of a quarter of the wavelength, $\lambda/4$. Such coatings can easily allow > 95% of the light to enter the PV cell at $\lambda$, but it is difficult to produce an anti-reflective coating that has high absorption over the whole of the spectrum of the sun.

The Shockley-Quessier limit is only for a single semiconductor material at 1 sun illumination. This efficiency can be increased if concentrators are used to increase the intensity of the light that impinges onto the PV cell surface. Concentrators can increase the maximum efficiency from roughly 31% at 1 sun to ~40% at 1000 suns illumination. A number of concentrator systems does operate with efficiencies well above the Shockley-Quessier limit of 31% for 1 sun [27].

The second approach to get efficiencies above the Shockley-Quessier limit is to use more than 1 semiconductor material with different bandgaps. Stacked systems with spectrally selective mirrors are one way to improve the spectral absorption and overall efficiency but such systems are much more expensive than multi-junction PV cells. Here, 1 or more semiconductors are epitaxially grown onto the one substrate to provide more than one bandgap for absorption. The widest bandgap material must be at the surface, and the record for a 5 junction solar cell is now 38.8% for 1 sun illumination and 46% with a 300 concentrator [27]. Whilst these recent results are now quite impressive, the multi-junction technology is predominantly with III-V materials and is therefore very expensive. It is not yet at the level to help to significantly reduce the cost per Watt which is key for applications and the market.

http://dx.doi.org/10.5772/65983

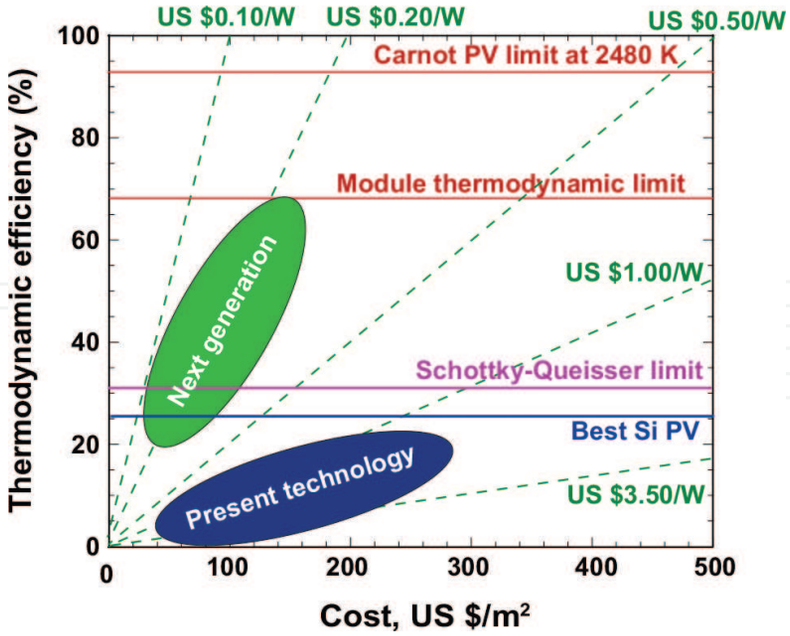


**Figure 17.** Graph showing the current density values as a function of $V_{oc}$ for different semiconductor materials.

**Figure 17** shows the cost of PV technology per unit area versus the efficiency. Also marked on the figure is the cost per Watt along with some of the key efficiencies for present Si PV, the Shockley-Quesser limit, the Carnot limit and the realistic module limit for multi-junction cells. Present crystalline Si, amorphous Si and other thin film technologies have efficiencies from 10 to 22% available on the market. For next generation technologies to have any major impact, they must manage to reduce the cost per Watt and also the capital cost of the PV technology per unit area. No technology has yet managed to achieve the low costs and the high efficiencies, so this is still a research area ripe for new technologies.

### 2.5. Applications

PV solar modules have a wide range of applications, many of which are well outside of ICT systems but also they can be used for powering a wide range of ICT systems.

- Large-scale solar farms for the powering of data centres and HPC clusters: 10 MW solar farms can certainly be built in appropriate environments, and many data centres already use the technology to reduce the carbon emissions. At present, the generation levels and poor large-scale electricity storage prevent 24/7 operation of the data centres from the PV renewable technology, and diesel generators or grid electricity are required for night operation when no solar energy is generating electricity.
- Small-scale ICT systems for indoor use such as calculators and digital watches: These applications have been around since the first products in the 1970s and can be enabled from the low-power requirements of the electronics.

- Rechargeable PV systems for mobile phones and larger ICT systems of the Watt and a few 10s Watt level: These are PV systems of 10–100 $cm^2$ which require direct sunlight to be able to generate the Whr required for ICT systems of the W to 10s Watt level. PV is really the only renewable or energy harvesting technology that can achieve power levels at the W level whilst thermoelectrics and vibrational systems have to be enormous and only really in industrial environments to be able to achieve power levels close to these values. Such PV systems can also recharge tablets and small laptops, but the charging time may be significant for the larger systems.
- Autonomous sensors both indoor but more frequently outdoor use PV cells with super capacitors or rechargeable batteries for continuous operation. Many road and rail warning and information signs as well as public information notices now use PV cells to provide a fit and forget technology to power the systems. Some building autonomous sensors for fire, smoke and temperature are now being sold with PV systems.
- Both industrial and domestic properties use PV to generate electricity. Whilst the amounts seldom are large enough to power the whole building, PV can generate sufficient energy to power a range of items in any building and in doing so be useful to reduce the load to the national grid and electricity generated from fossil fuels. In many cases, it is sensible to power ICT devices as these require DC power, and the DC generation from the PV does not require to be converted to ac and then back to DC with the combined losses in both conversion processes. In many countries, feed-in tariffs have been used to subsidise the large capital costs to enable countries to significantly increase their renewable energy generation capacity.

## 3. Thermal photovoltaics (TPV)

It is clear that neither thermoelectrics nor photovoltaics are operated anywhere close to the Carnot limit for thermodynamic conversion (see **Figures 2**and **17**). Therefore, both systems have significant losses which result in heat. A secondary issue is that the thermal to electrical conversion efficiency of photovoltaics decreases as the temperature is increased. For example, a crystalline Si PV cell reduces in efficiency by about 0.4% per 1°C rise [28]. Therefore, there has been an interest in combining photovoltaics and thermoelectrics together in the field of thermal photovoltaics (TPV). The whole of the TPV field is much larger than just PV combined with thermoelectrics and includes thermal heating for combined heat and power systems especially for integrated modules into buildings where the heat is used either to produce hot water for a property or to heat the building [28]. A number of PVT technology is optimised to maximise the heating element which is not appropriate for ICT systems. Here, we will restrict the use to energy harvesting scenarios which are optimised and appropriate for providing electricity to ICT devices and systems. With this proviso, the range of PVT technologies which are useful reduces dramatically as a key part must be the production of electricity.

As has been discussed with PV, concentrators allow significant improvements in the efficiency and output power. Whilst improvements are obtained with single junction technology, the largest power outputs are obtained with concentrator-based multi-junction PV. Such technologies are not appropriate for miniature portable PV systems but tend to be more appropriate for

http://dx.doi.org/10.5772/65983

large-scale solar farms, many of which are used with HPC or data centres. Whilst the concentration increases the conversion efficiency per unit area and increases the output power, the disadvantage is the significant increase in operating temperature of the PV which both reduces efficiency and can also lead to failures through repeated thermal expansion and contraction. The thermal cycling failures can be more significant where ice formation at night can occur since the volume of ice is significantly larger than an equivalent mass of water leading to significant mechanical damage if the ice grows in particular ways around PV modules. Therefore, one form of TPV is to use a thermal store with a heat pump such as a thermoelectric to reduce the temperature of the PV section thereby increasing the efficiency but then storing this heat energy during the day. Heat is pumping back to the PV at night to reduce the probability of ice formation and failures from thermal contraction.

The most common form of a PVT generator at present is a PV cell with a fluid-based system to conduct the heat away from the cell to use for heating buildings or hot water systems. The best of these systems have an overall efficiency approaching 70% with about 20% electrical efficiency and over 50% thermal efficiency. The priority for ICT applications similar to most of these PVT systems is the electrical output. The real problem, however, is that this is a classic example of the quality of energy: the conversion efficiencies of low grade energy can be significantly higher than those for high-quality energy such as electricity. At present, few of the PVT systems use thermoelectrics to generate electricity, as the thermoelectric output is so low, but this may be a possibility in the future for ICT systems where the use of heat is not required.

## 4. Conclusions

To conclude, the fundamental operation and efficiency of thermoelectrics, photovoltaics and thermal photovoltaics have been reviewed. For each of the technologies, ICT applications have been described, and some of the problems have also been discussed. It is clear that these technologies are key to enable renewable sources of electricity to power ICT systems in the future if carbon emissions are to be reduced. These research fields are very active as all the technologies at present are still too expensive both in terms of capital cost and the cost per Watt of electricity generated compared to batteries and fossil-fuel-based grid electricity. Such systems are starting to be implemented where carbon taxes or subsidies can overcome the large capital investment barriers or companies are prepared to have long payback times before significant cost reductions can be achieved. As none of the technologies are close to the Carnot thermodynamic limit, there is the potential for substantial improvement in the future.

## Author details

Lourdes Ferre Llin and Douglas J. Paul*

*Address all correspondence to: Douglas.Paul@glasgow.ac.uk

School of Engineering, University of Glasgow, Glasgow, UK

## References


[1] Harrop., The hot applications for energy harvesting (2009). http://www.energyharvestingjournal.com/articles/the-hot-applications-for-energy-harvesting-00001247.asp

[2] H.J. Goldsmid, *Introduction to Thermoelectricity* (Springer-Verlag, Berlin Heidelberg, 2010)

[3] D.M. Rowe, *Thermoelectrics Handbook: Macro to Nano* (CRC Taylor and Francis, Boca Raton Florida, 2006)

[4] G.J. Snyder, E.S. Toberer, Nature Materials **7**(2), 105 (2008)

[5] J. Dismukes, E. Ekstrom, D. Beers, E. Steigmeier, I. Kudman, Journal of Applied Physics **35**(10), 2899 (1964)

[6] R. Venkatasubramanian, E. Siivola, T. Colpitts, B. O'Quinn, Nature **413**(6856), 597 (2001)

[7] A.I. Boukai, Y. Bunimovich, J. Tahir-Kheli, J.K. Yu, W.A. Goddard, J.R. Heath, Nature **451** (7175), 168 (2008)

[8] G. Joshi, H. Lee, Y.C. Lan, X.W. Wang, G.H. Zhu, D.Z. Wang, R.W. Gould, D.C. Cuff, M.Y. Tang, M.S. Dresselhaus, G. Chen, Z.F. Ren, Nano Letters **8**(12), 4670 (2008)

[9] Y. Ma, Q. Hao, B. Poudel, Y. Lan, B. Yu, D. Wang, G. Chen, Z. Ren, Nano Letters **8**(8), 2580 (2008)

[10] Q. Zhang, J. He, T.J. Zhu, S.N. Zhang, X.B. Zhao, T.M. Tritt, Applied Physics Letters **93** (10), 102109 (2008)

[11] T.C. Harman, P.J. Taylor, M.P. Walsh, B.E. LaForge, Science **297**(5590), 2229 (2002)

[12] X.W. Wang, H. Lee, Y.C. Lan, G.H. Zhu, G. Joshi, D.Z. Wang, J. Yang, A.J. Muto, M.Y. Tang, J. Klatsky, S. Song, M.S. Dresselhaus, G. Chen, Z.F. Ren, Applied Physics Letters **93** (19), 193121 (2008)

[13] T. Harman, M. Walsh, B. laforge, G. Turner, Journal of Electronic Materials **34**, L19 (2005)

[14] Micropelt (2016). URL http://www.micropelt.com/

[15] C. Watkins, B. Shen, R. Venkatasubramanian, in *Thermoelectrics, 2005. ICT 2005. 24th International Conference on* (2005), pp. 265–267

[16] J. Yang, F.R. Stabler, Journal of Electronic Materials **38**(7), 1245 (2009)

[17] G. Pearson, W.H. Brattain, Proceedings of the Institute of Radio Engineers **43**, 1794 (1955)

[18] S.M. Sze, *Physics of Semiconductor Devices* (John Wiley and Sons, New York, 1981)

[19] E. Bequerel, Compter Rendues **9**, 561 (1839)

[20] W.G. Adams, R.E. Day, Proceedings of the Royal Society A25, 113 **A25**, 113 (1877)

[21] W. Shockley, The Bell System Technical Journal **28**, 435 (1949)

[22] D.M. Chapin, C. Fuller, G. Pearson, Journal of Applied Physics **25**, 676 (1954)

[23] Y. Chevalier, F. Duenas, in *Proceedings of 2nd European Conference on Photovoltaics Solar Energy*, vol. 2 (1979), pp. 817–823

[24] Photovoltaics report (2016). URL https://www.ise.fraunhofer.de/de/downloads/pdf-files/aktuelles/photovoltaics-report-in-englischer-sprache.pdf

[25] R. Pierret, G. Neudeck, *The P-N Junction Diode* (Addison and Wesley, Reading MA, 1994)

[26] W. Shockley, H.J. Queisser, Journal of Applied Physics **32**(3), 510 (1961)

[27] M.A. Green, K. Emery, Y. Hishikawa, W. Warta, E.D. Dunlop, Progress in Photovoltaics: Research and Applications **23**(1), 1 (2015)

[28] T. Chow, Applied Energy **87**(2), 365 (2010)

IntechOpen